Pergamon

Int. J. Heat Mass Transfer. Vol. 40, No. 17, pp. 4183–4190, 1997

Printed in Great Britain
0017–9310/97 $17.00+0.00

PII: S0017–9310(97)00029–X

New logarithmic technique in the flash method

MARC-ANTOINE THERMITUS and MICHEL LAURENT
CETHIL INSA-Lyon, 20 Av. A. Einstein, 69621 Villeurbanne, France

(*Received* 7 *June* 1996 *and in final form* 10 *December* 1996)

Abstract—The logarithmic transformation of the rear face temperature rise issued from a flash experiment can be interpreted as adding up a heat loss and radial effect component to the one for the adiabatic model. Two data reduction methods based on this transformation are proposed with the common main goal to identify one parameter depending upon the sample's thickness and thermal diffusivity, not upon the other experimental conditions. They allow one to determine thermal diffusivity with good accuracy for non-uniform pulses and high Biot numbers. © 1997 Elsevier Science Ltd.

1. INTRODUCTION

The flash experiment introduced by Parker *et al.* [1] has become widely used. In this method, a cylindrical sample absorbs a short energy pulse on the front face and the resulting rear face temperature rise is analysed to determine the thermal diffusivity. The original method assumes ideal conditions of uniform and instantaneous energy pulse, homogeneous, isotropic and opaque sample, adiabatic boundaries, one-dimensional (1D) heat diffusion and constant thermophysical properties within the temperature rise. Several data reduction methods have been proposed over the years to account for heat losses [2–9] and finite pulse width [10, 11].

Another approach is the logarithmic method [12]. It also assumes ideal conditions and uses Laplace transform and term by term inversion to the time domain. The obtained relation has the peculiarity of being less sensitive to heat losses and non-uniformity of the pulse at the early stage of the temperature rise. Thermal diffusivity can be determined with good accuracy up to 1000 K. However, with increasing temperature and for samples with low thermal conductivity, the identification errors become significant. The purpose of this paper is to enhance this method providing a new regression model.

2. LOGARITHMIC APPROXIMATION

Consider a cylindrical sample of thickness L, radius R, density ρ, specific heat C_p, conductivity λ, diffusivity α, uniform initial temperature T_0 and absorbing a pulse of energy Q at the front face. The dimensionless temperature under ideal conditions is given by [1]:

$$\theta_1^*(z^*, t^*) = 1 + 2\sum_{n=1}^{\infty} \cos(n\pi z^*) \exp(-n^2\pi^2 t^*) \quad (1)$$

where $z^* = z/L$, $t^* = \alpha t/L^2$ (Fourier number) and $\theta_1^* = \rho C_p L(T-T_0)/Q$.

In the case of a non-uniform pulse and heat transfer between the sample and the environment, the heat diffusion model becomes two-dimensional (2D). The dimensionless solution obtained using Green's functions or the method of separation of variable can be written as the product of two components, θ_z^* (axial component) and θ_r^* (radial component) [13, 14]:

$$\theta_2^*2(z^*, r^*, t^*) = \theta_z^*(z^*, t^*) \times \theta_r^*(r^*, t^*) \quad (2)$$

where

$$\theta_z^*(z^*, t^*) = \sum_{m=1}^{\infty} \frac{2\eta_m^2(\eta_m^2 + Bi_L^2)[\cos(\eta_m z^*) + Bi_0 \sin(\eta_m z^*)/\eta_m]}{(\eta_m^2 + Bi_0^2)(\eta_m^2 + Bi_L^2) + (Bi_0 + Bi_L)(\eta_m^2 + Bi_0 Bi_L)} \times \exp(-t^*\eta_m^2) \quad (3)$$

$$\theta_r^*(r^*, t^*) = \sum_{p=1}^{\infty} \frac{2\gamma_p^2 J_0(\gamma_p r^*/R^*)}{R^{*2} J_0^2(\gamma_p)(Bi_R^2 R^{*2} + \gamma_p^2)} \times \int_0^{R^*} r' J_0(\gamma_p r'/R^*) f(r')\, dr' \exp(-t^*\gamma_p^2/R^{*2}) \quad (4)$$

and $r^* = r/L$, $R^* = R/L$, $Bi_0 = h_0 L/\lambda$ (Biot number on the front face), $Bi_L = h_L/\lambda$ (Biot number on the rear face), $Bi_R = h_R L/\lambda$ (Biot number on the lateral face) and $f(r')$ the energy density distribution of the pulse. η_m and γ_p are, respectively, positive roots of:

$$\tan(\eta) = \frac{\eta(Bi_0 + Bi_L)}{\eta^2 - Bi_0 Bi_L} \quad (5)$$

$$\gamma J_1(\gamma) = Bi_R R^* J_0(\gamma). \quad (6)$$

Let Θ_1^* and Θ_2^* be defined for the thermograms at the center of the rear face ($z^* = 1$ and $r^* = 0$):

$$\Theta_1^*(t_1^*) = \ln(\theta_1^*(1, t^*)\sqrt{t^*}) \quad (7)$$

$$\Theta_2^*(t_1^*) = \ln(\theta_2^*(1, 0, t^*)\sqrt{t^*}) \quad (8)$$

NOMENCLATURE

B	constant
Bi	Biot number
C_p	specific heat
EKF	extended Kalman filter
I_0, I_1	modified Bessel functions
J_0, J_1	first kind Bessel functions
L	sample thickness
LM	Levenberg–Marquardt
Q	absorbed energy
r	radial coordinate
R	sample radius
t	time
t_i	inverse time
T	temperature
T_0	initial temperature
x	state
$\mathbf{X}$	state vector
y	measurement
z	axial coordinate.

Greek symbols

α	thermal diffusivity
ε	measurement noise
Γ	Gamma function
λ	thermal conductivity
ρ	density
θ	temperature
Θ	logarithmic transform.

Subscripts

0	frontface
1	ideal conditions
2	heat loss
$2s$	heat loss (short times)
L	rear face
r	radial component
R	lateral face
z	axial component.

Superscripts

*	dimensionless
^	estimated
~	Laplace transform
T	transpose.

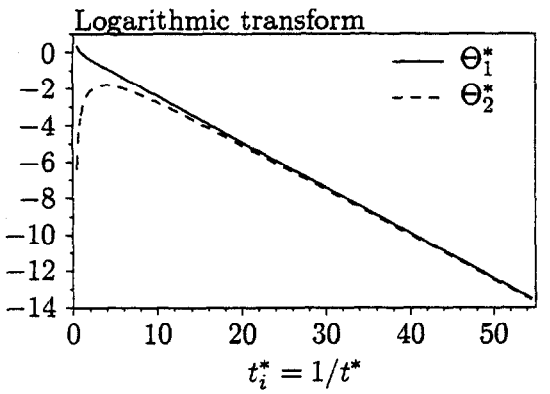

Fig. 1. Functions Θ_1^* and Θ_2^* (Θ_2^* computed for $Bi = 1$ and $R^* = 1$).

with $t_i^* = 1/t^*$ and $Bi_0 = Bi_L = Bi_R = Bi$. This formulation is referred to as "logarithmic transformation".

As shown in Fig. 1, the monotonously decreasing part of Θ_1^* is similar to a straight line. The standard logarithmic method suitable for low heat loss takes advantage of this characteristic [12]. However, with increasing heat loss, the transform Θ_2^* becomes quite different. Another approximation is, therefore, required.

The first step to this end is to find a new solution of the 2D model. Unlike θ_2^*, this solution must converge at small times with only few terms. Using the Green's function obtained with the Laplace transform method [13], the axial component θ_z^* becomes:

$$\theta_z^*(z^*, t^*) = \frac{1}{\sqrt{\pi t^*}} \exp\left(-\frac{z^{*2}}{4t^*}\right) + \frac{1}{\sqrt{\pi t^*}} \exp\left(-\frac{(2-z^*)^2}{4t^*}\right) - Bi_0 \exp(Bi_0 z^* + Bi_0^2 t^*) \times \operatorname{erfc}\left(Bi_0\sqrt{t^*} + \frac{z^*}{\sqrt{4t^*}}\right) - Bi_L \exp(Bi_L(2-z^*) + Bi_L^2 t^*) \times \operatorname{erfc}\left(Bi_L\sqrt{t^*} + \frac{2-z^*}{\sqrt{4t^*}}\right) + , \cdots . \quad (9)$$

In the case of an uniform pulse, the radial component of the temperature at the center of the rear face can be approximated with an exponential function for small values of t^* (refer to Appendix A for more details):

$$\theta_r^*(0, t^*) = \exp(-B(\alpha t/R^2)^2) + , \cdots ,$$
$$\theta_r^*(0, t^*) = \exp\left(-\frac{B}{R^{*4}} t^{*2}\right) + , \cdots . \quad (10)$$

Although the exponential approximation has been theoretically derived for $r^* = 0$ and $f(r^*) = 1$, it also

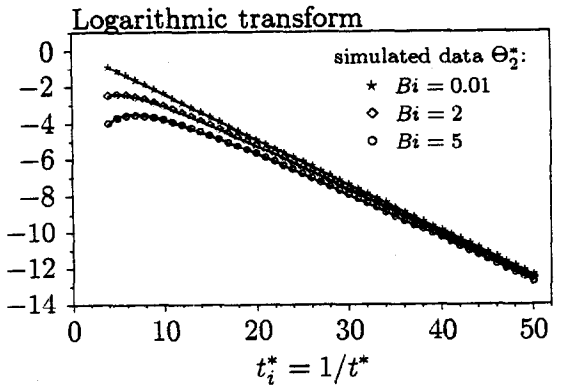

Fig. 2. Functions $\Theta_{2,}^*$ (continuous curves) obtained by identifying Bi and B_1 from values of Θ_2^* ($R^* = 1$).

applies to cases where these conditions are not satisfied (Section 3.1).

Analogous to Θ_2^*, the function Θ_{2s}^* is defined as:

$$\Theta_{2s}^*(t_i^*) = \ln[\theta_z^*(1, t^*)\theta_r^*(0, t^*)\sqrt{t^*}]$$
$$= \ln\left[\frac{2}{\sqrt{\pi}}\exp\left(-\frac{t_i^*}{4}\right)\right.$$
$$\times\left(1 - Bi\sqrt{\frac{\pi}{t_i^*}}\exp\left(\frac{2Bi + t_i^*}{2\sqrt{t_i^*}}\right)^2\right.$$
$$\left.\left.\times\operatorname{erfc}\left(\frac{2Bi + t_i^*}{2\sqrt{t_i^*}}\right)\right)\exp\left(-\frac{B}{R^{*4}t_i^{*2}}\right)\right] \quad (11)$$

with $Bi_0 = Bi_L = Bi_R = Bi$. For large values of t_i^* i.e. small Fourier numbers, the first-order asymptotic expansion of the error function gives [15]:

$$\operatorname{erfc}\left(\frac{2Bi + t_i^*}{2\sqrt{t_i^*}}\right) \approx \exp\left(-\left(\frac{2Bi + t_i^*}{2\sqrt{t_i^*}}\right)^2\right)\frac{1}{\sqrt{\pi}}\frac{2\sqrt{t_i^*}}{2Bi + t_i^*}. \quad (12)$$

According to equations (11) and (12), Θ_{2s}^* becomes:

$$\Theta_{2s}^*(t_i^*) = \underbrace{-\frac{t_i^*}{4} + \ln\left(\frac{2}{\sqrt{\pi}}\right)}_{\text{adiabatic sample}}$$
$$\underbrace{-\left(\frac{B}{R^{*4}t_i^{*2}} - \ln\left(\frac{t_i^*}{2Bi + t_i^*}\right)\right)}_{\text{heat loss and radial effect}}. \quad (13)$$

The same adiabatic term is used in the standard logarithmic method. The new additional component enables Θ_{2s}^* to match several experimental conditions such as high Biot numbers (Fig. 2). Therefore, Θ_{2s}^* is a fairly good approximation of Θ_2^*.

3. IDENTIFICATION OF THE THERMAL DIFFUSIVITY

Under the assumption of no measurement noise, the data resulting from a flash experiment can be thought of as given by equation (2). Letting $\theta_{2s}^* \to \theta_{2s}/\theta_m$ and $t_i^* \to L^2 t_i/\alpha$, equation (13) yields to:

$$\ln(\theta_{2s}(t)\sqrt{t}) = -\frac{L^2}{4\alpha}t_i - \frac{B\alpha^2}{R^{*4}L^4}\frac{1}{t_i^2}$$
$$+\ln\left(\frac{2\theta_m L}{\sqrt{\pi\alpha}}\frac{L^2 t_i/\alpha}{2Bi + L^2 t_i/\alpha}\right) \quad (14)$$

where $t_i = 1/t$ and $\theta_m = Q/\rho C_p L$.

This equation can be rewritten in order to express four governing parameters C_1, C_2, C_3 and C_4:

$$\Theta_{2s}(t_i) = \ln(\theta_{2s}(t)\sqrt{t}) \quad (15)$$

$$\Theta_{2s}(t_i) = -C_1 t_i - C_2\frac{1}{t_i^2} + \ln\left(C_3\frac{t_i}{C_4 + t_i}\right). \quad (16)$$

Notice that C_1 is the slope of Θ_{2s} at short times. It is equivalent to the slope of a straight line for an adiabatic sample absorbing an uniform pulse. It does not depend on heat loss or radial effect and, hence, is the only one parameter to be determined with best accuracy.

Equation (16) assumes that the pulse is instantaneous. The unavoidable finite pulse width in a practical experiment can be compensated with the correction method of center of gravity [10, 11].

3.1. *Identification with the Levenberg–Marquardt method (LM)*

As shown in Fig. 3, the high sensibility of Θ_{2s} to C_1 at short times reveals the great significance of the early stage of the thermogram. On the contrary, in this interval, the sensibilities to the other parameters are relatively low and almost linear dependent. This is a typical case to use the Levenberg–Marquardt method which may converge for such an ill-posed problem [16, 17]. Once $C_1, \ldots, C_4$ have been identified, the thermal diffusivity is obtained from C_1 with:

$$\alpha = \frac{L^2}{4C_1}. \quad (17)$$

In Tables 1 and 2 are reported the relative identi-

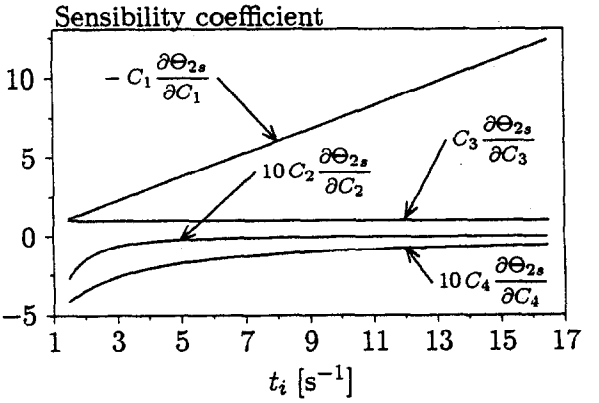

Fig. 3. Sensibility coefficients of Θ_{2s}.

Table 1. Relative identification errors of thermal diffusivity for an uniform pulse: comparison between the Levenberg–Marquardt and moment methods. No measurement noise and moment method adapted to $R^* = 1$ (Appendix B)

	Levenberg–Marquardt			Moment method†		
	$r^* = 0$ [%]	$r^* = 0.1$ [%]	$0 \leqslant r^* \leqslant 0.1$ [%]	$r^* = 0$ [%]	$r^* = 0.1$ [%]	$0 \leqslant r^* \leqslant 0.1$ [%]
$Bi = 0.05$	0.01	0.01	0.01	0.00(0.17)	0.01(0.17)	0.00(0.17)
$Bi = 0.8$	0.05	0.03	0.04	0.02(3.03)	0.08(2.96)	0.04(2.99)
$Bi = 3$	0.11	0.07	0.09	0.02(5.02)	0.10(4.92)	0.05(4.97)

† Values in parentheses obtained according to [9].

Table 2. Relative identification errors of thermal diffusivity for a gaussian pulse: comparison between the Levenberg–Marquardt and moment methods. No measurement noise and moment method adapted to $R^* = 1$ (Appendix B)

	Levenberg–Marquardt			Moment method†		
	$r^* = 0$ [%]	$r^* = 0.1$ [%]	$0 \leqslant r^* \leqslant 0.1$ [%]	$r^* = 0$ [%]	$r^* = 0.1$ [%]	$0 \leqslant r^* \leqslant 0.1$ [%]
$Bi = 0.05$	0.08	0.14	0.11	17.87(17.75)	17.35(17.23)	17.61(17.49)
$Bi = 0.8$	0.49	0.46	0.47	9.98(6.46)	9.86(6.33)	9.91(6.40)
$Bi = 3$	1.35	1.32	1.33	6.12(0.80)	6.04(0.73)	6.08(0.77)

† Values in parentheses obtained according to [9].

fication errors of the Levenberg–Marquardt method in comparison to those of the moment method [9] for a sample with $\alpha = 9.2 \times 10^{-6}$ m^2 s^{-1} and $R = L = 6$ mm (no measurement noise). Different measurement locations are considered: at the center of the rear face ($r^* = 0$), beside the center ($r^* = 0.1$) and mean temperature over a circular surface around the center ($0 \leqslant r^* \leqslant 0.1$). The comparison is mainly made with the moment method adapted to $R^* = 1$ (Appendix B) while the new regression model (equation (16)) does not place any restriction on R^*.

Table 1 shows that both methods are relatively unaffected by heat losses and the exact measurement location. Unlike the Levenberg–Marquardt method, the moment method achieves this result at high Biot numbers only if it is adapted to the actual dimensionless radius R^* of the sample. Furthermore, the new regression model is, by far, less sensitive to the non-uniformity of the pulse. In the case of a gaussian pulse, whose intensity at the external radius of the sample falls to 13.5% of its axial value, the errors remain low, due to the ability of parameters $C_2, \ldots, C_4$ to carry over radial effects (Table 2). This underlines the adequacy of Θ_{2s} when flash experiments are made with a laser beam which often exhibits a gaussian transverse irradiance profile.

Under real conditions, the measurements are always corrupted with noise $\varepsilon(t)$ supposed to be stationary, additive, gaussian, white and zero-mean. Because of the logarithmic transformation, the perturbations are no longer equally distributed and become very significant at short times (Fig. 4). The identification will be achieved either by neglecting the strong dispersed data or, eventually, by including some general information in a weighting matrix.

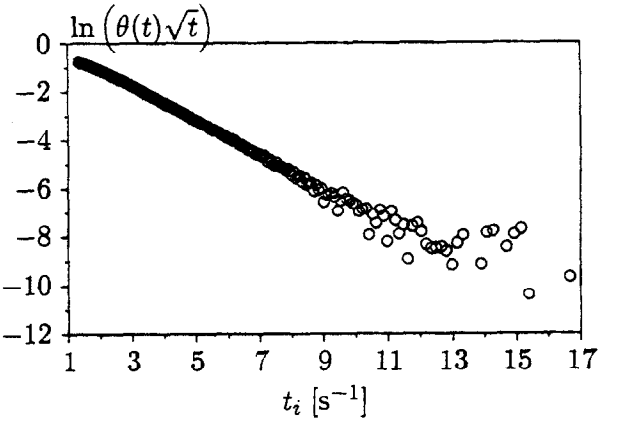

Fig. 4. Logarithmic transform of noisy simulated data (noise standard deviation: $\theta_{max}/100$).

The identification process is then organised in the following steps:

(i) Selection of the rising part of the thermogram.

(ii) Elimination of the part containing negative or null values, owing to the properties of the logarithmic function.

(iii) Logarithmic transformation of the selected data:

$$(t_j, \theta_j) \rightarrow (1/t_j, \ln(\theta_j \sqrt{t_j})).$$

(iv) Approximative estimation of C_1 with the standard logarithmic method.

(v) Eventually, establishment of a weighting matrix to minimize the importance of strong dispersed data.

(vi) Estimation of C_1, C_2, C_3 and C_4 with the Lev-

enberg–Marquardt method based on the new regression model (equation (16)).

(vii) Computation of the thermal diffusivity with equation (17).

3.2. *Identification with the extended Kalman filter (EKF)*

The parameter estimation in the previous section was performed from a logarithmic, i.e. non-linear transformation of the recorded data. Therefore, the assumptions on the statistical characteristics of the measurement noise $\varepsilon(t)$ cannot be taken into account and, thus, there is no guarantee for the Levenberg–Marquardt estimator to be optimal. On the other hand, it is not possible to derive full benefit from the data at short times. Using the extended Kalman filter as a parameter identifier allows to avoid this negative effect provided Θ_{2s} is given in state form.

Assuming that the thermogram is recorded at small enough time intervals, the first-order Taylor expansion of equation (16) gives:

$$\Theta_{2s}(t_k) = \Theta_{2s}(t_{k-1}) + (t_k - t_{k-1}) \left.\frac{d\Theta_{2s}}{dt}\right|_{t_{k-1}} . \quad (18)$$

The state x of the model corresponds to Θ_{2s}. It is related to the measurements y according to equation (20). The resulting state (process-measurement) model is given as:

$$x_k = x_{k-1} + \frac{t_k - t_{k-1}}{t_{k-1}^2}\left(\frac{L^2}{4\alpha} - 2C_2 t_{k-1}^3 - \frac{C_4 t_{k-1}^2}{C_4 t_{k-1} + 1}\right) \quad (19)$$

$$y_k = \frac{1}{\sqrt{t_k}} \exp(x_k) + \varepsilon_k . \quad (20)$$

The parameter C_3 has no influence on the process evolution. This state formulation simply provides the possibility of taking advantage of the logarithmic transformation, while keeping track of the measurement noise characteristics. Three parameters are now to be determined: α, C_2 and C_4. Consider the state vector $\mathbf{X} = [x, \alpha, C_2, C_4]^T$. The new state model becomes:

$$\begin{bmatrix} x_k \\ \alpha_k \\ C_{2,k} \\ C_{4,k} \end{bmatrix} = \begin{bmatrix} x_{k-1} + \dfrac{t_k - t_{k-1}}{t_{k-1}^2}\left(\dfrac{L^2}{4\alpha} - 2C_{2,k-1} t_{k-1}^3 - \dfrac{C_{4,k-1} t_{k-1}^2}{C_{4,k-1} t_{k-1} + 1}\right) \\ \alpha_{k-1} \\ C_{2,k-1} \\ C_{4,k-1} \end{bmatrix} \quad (21)$$

$$y_k = \frac{1}{\sqrt{t_k}} \exp(x_k) + \varepsilon_k \quad (22)$$

or simply

$$\begin{cases} \mathbf{X}_k = \mathbf{F}(\mathbf{X}_{k-1}) \\ y_k = H(\mathbf{X}_k) + \varepsilon_k \end{cases} \quad (23)$$

where $\mathbf{F}$ and H are non-linear vector functions defined in equations (21) and (22).

The state vector estimation will be achieved with the extended Kalman filter proceeding the data recursively [18]. At each recursion, the model is linearised about the state vector of the previous step and the updated estimate $\hat{\mathbf{X}}$ is obtained according to:

$$\hat{\mathbf{X}}_{k|k-1} = \mathbf{F}(\hat{\mathbf{X}}_{k-1|k-1}) \quad \text{state prediction}$$

$$\mathbf{P}_{k|k-1} = \mathbf{A}(\hat{\mathbf{X}}_{k|k-1})\mathbf{P}_{k-1|k-1}\mathbf{A}^T(\hat{\mathbf{X}}_{k|k-1}) \quad \text{covariance prediction}$$

$$e_k = y_k - H(\hat{\mathbf{X}}_{k|k-1}) \quad \text{innovation}$$

$$W_k = \mathbf{H}(\hat{\mathbf{X}}_{k|k-1})\mathbf{P}_{k|k-1}\mathbf{H}^T(\hat{\mathbf{X}}_{k|k-1}) + V_k \quad \text{innovation covariance}$$

$$\mathbf{K}_k = \mathbf{P}_{k|k-1}\mathbf{H}^T(\hat{\mathbf{X}}_{k|k-1}) W_k^{-1} \quad \text{Kalman gain}$$

$$\hat{\mathbf{X}}_{k|k} = \hat{\mathbf{X}}_{k|k-1} + \mathbf{K}_k e_k \quad \text{state correction}$$

$$\mathbf{P}_{k|k} = [\mathbf{I} - \mathbf{K}_k \mathbf{H}(\hat{\mathbf{X}}_{k|k-1})]\mathbf{P}_{k|k-1} \quad \text{covariance correction} \quad (24)$$

with

$$\hat{\mathbf{X}}_{0|0} = E(\mathbf{X}_0) \quad \text{initial state vector}$$

$$\mathbf{P}_{0|0} = \mathrm{Cov}(\mathbf{X}_0) \quad \text{initial covariance matrix}$$

$$V_k \delta_{kj} = E(\varepsilon_k \varepsilon_j) \quad \text{measurement noise variance}$$

$$\mathbf{A} = \left[\frac{\partial F_i}{\partial X_j}\right] \quad \text{jacobian matrix of } \mathbf{F}$$

$$\mathbf{H} = \left[\frac{\partial H}{\partial X_j}\right] \quad \text{jacobian vector of } \mathbf{H}.$$

The components of the initial state vector can be obtained with the method described in the previous section. The initial state covariance matrix $\mathbf{P}_{0|0}$ is diagonal with values set large enough in order to affect the transient performance of the algorithm, i.e. to optimize the significance of the measurements at short times.

A necessary and sufficient condition for the Kalman filter to be optimal is that the innovation sequence $\{e_k\}$ is zero-mean and white [18]. These properties must be evaluated to ensure that the estimator is operating properly and, eventually, to adjust the initial parameter estimates and the variance V_k when no information about the measurements is available.

4. RESULTS AND DISCUSSION

Figure 5 depicts an example of thermal diffusivity determination with the extended Kalman filter. The thermogram was simulated with the following values: uniform pulse, $\alpha = 9.2 \times 10^{-6}$ m^2 s^{-1}, $L = 6$ mm, $R = 6$ mm, $Bi = 0.8$ and noise $\varepsilon(t)$ gaussian, zero-mean with standard deviation $\theta_{max}/200$. Owing to the high sensibility to C_1 at short times, the thermal diffusivity estimate already converges after few measurements (Fig. 5b). On the contrary, the C_2 and C_4 estimates do not converge (Fig. 6), however, without any effect on the evolution of the thermal diffusivity. The innovation sequence is statistically zero-mean and white (Fig. 7). Thus, the minimum variance estimate of the thermal diffusivity is $\hat{\alpha} = 9.22 \times 10^{-6}$ m^2 s^{-1} with the 95% confidence interval: 9×10^{-8} m^2 s^{-1}. The effectiveness of this bound was attested with the Monte-Carlo technique (100 runs).

Table 3 reports the mean relative errors obtained with different identification methods for the same sample as above. Each mean value was computed over a set of 100 simulated gaussian and additive noise of equal standard deviation. Unlike the state model, the regression model used in the Levenberg–Marquardt method is strongly sensible to measurement noise at short times (Sections 3.1 and 3.2). This explains the better performance of the EKF identifier.

5. CONCLUSION

A new regression method based on the logarithmic transformation of the thermogram has been proposed. It has the peculiarity of being less sensitive to heat loss and radial diffusion. Among the four governing parameters, only one solely depends on the thermal diffusivity, the others ensuring the adequacy of the model with the experimental conditions, i.e. sample's radius, measurement location, Biot number and non-uniformity of the pulse. The determination of the maximal temperature rise and partial times, which often brings up errors in other methods, is not required.

The use of the Kalman filter as a parameter identifier allows one to avoid the high sensitivity of the logarithmic transformation to measurement noise at the early stage of the thermogram. Thermal diffusivity can then be determined with best accuracy at high temperatures or for material with low thermal conductivity.

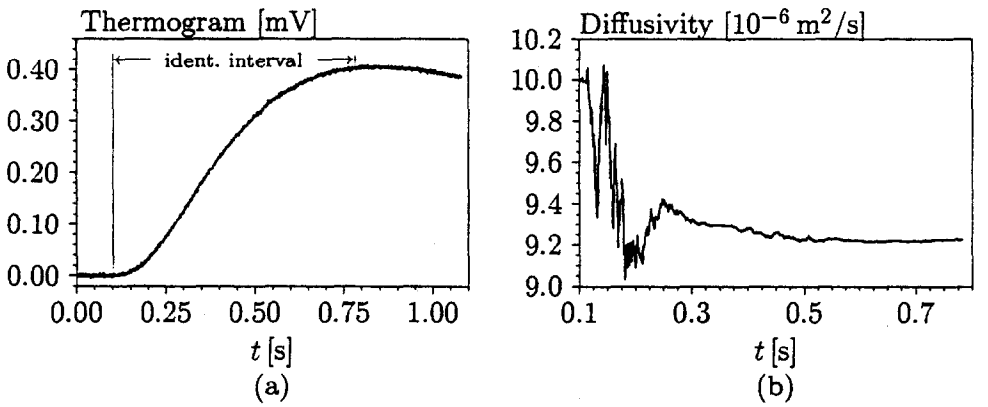

Fig. 5. Extended Kalman filter: (a) simulated temperature rise; (b) recursive identification of the thermal diffusivity.

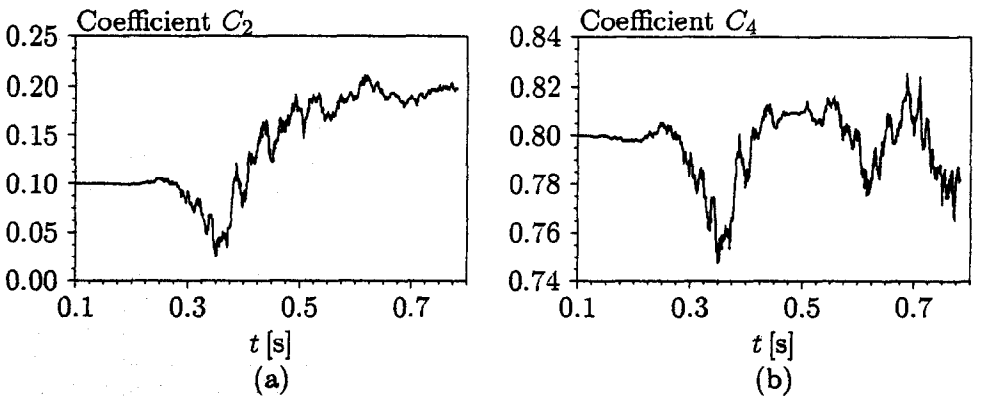

Fig. 6. Extended Kalman filter: (a) recursive identification of C_2; (b) recursive identification of C_4.

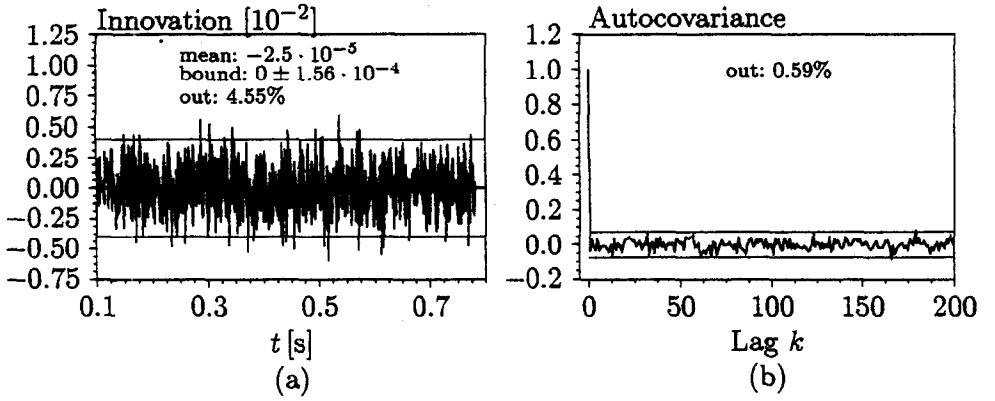

Fig. 7. Extended Kalman filter: (a) innovation sequence; (b) whiteness test.

Table 3. Relative identification errors of thermal diffusivity for various Biot numbers and noise standard deviations (uniform pulse and $R^* = 1$)

	$Bi = 0.1$		$Bi = 1$	
	$\theta_{max}/100$ [%]	$\theta_{max}/20$ [%]	$\theta_{max}/100$ [%]	$\theta_{max}/20$ [%]
Moment method (Appendix B)	0.72	1.05	0.75	1.09
Standard logarithmic [12]	2.45	4.75	12.55	13.84
Levenberg–Marquardt	1.62	3.65	2.17	4.12
Extended Kalman filter	0.70	0.85	0.72	0.97

REFERENCES

1. Parker, W. J., Jenkins, R. J., Butler, C. P. and Abbot, G. L., Flash method of determining thermal diffusivity, heat capacity and thermal conductivity. *Journal of Applied Physics*, 1961, **32**, 1679–1684.
2. Parker, W. J. and Jenkins, R. J., Thermal conductivity measurements on bismuth telluride in the presence of a 2 MeV electron beam. *Advanced Energy Conversion*, 1962, **2**, 87–103.
3. Cowan, R. D., Pulse method of measuring thermal diffusivity at high temperatures. *Journal of Applied Physics*, 1961, **34**, 926–927.
4. Cape, J. A. and Lehman, G. W., Temperature and finite pulse time effects in the flash method for measuring thermal diffusivity. *Journal of Applied Physics*, 1963, **34**, 1909–1913.
5. Clark III, L. M. and Taylor, R. E., Radiation loss in the flash method for measurement of thermal diffusivity. *Journal of Applied Physics*, 1975, **46**, 714–718.
6. Balageas, D. L., Nouvelle méthode d'interprétation des thermogrammes pour la détermination de la diffusivité thermique par la méthode impulsionnelle (méthode "flash"). *Review of Physics Applications*, 1982, **17**, 227–237.
7. Raynaud, M., Beck, J. V., Shoemaker, R. and Taylor, R. E., Sequential estimation of thermal diffusivity for flash tests. In *Thermal Conductivity* 20. Plenum Press, New York, 1989, pp. 305–321.
8. Degiovanni, A., Diffusivité et méthode flash. *Revue Générale Thermique*, 1977, **185**, 420–441.
9. Degiovanni, A. and Laurent, M., Une nouvelle technique d'identification de la diffusivité thermique par la méthode flash. *Review of Physics Applications*, 1986, **21**, 229–237.
10. Azumi, T. and Takahashi, Y., Novel finite pulse-width correction in flash thermal diffusivity measurement. *Review of Science Instruments*, 1981, **52**, 1411–1413.
11. Degiovanni, A., Correction de longueur d'impulsion pour la mesure de la diffusivité thermique par la méthode flash. *International Journal of Heat and Mass Transfer*, 1987, **30**, 2199–2200.
12. Takahashi, Y., Yamamoto, K., Ohsato, T. and Terai, T., Usefulness of logarithmic method in laser-flash technique for thermal diffusivity measurement. *Proceedings of the 9th Japanese Symposium on Thermophysical Properties*, 1988, pp. 175–178.
13. Beck, James V., Cole, Kevin D., Haji-Sheikh, A. and Litkouhi Bahman, *Heat Conduction Using Green's Functions*. Hemisphere, Washington, D.C., 1992.
14. Necati Özişik, M., *Heat Conduction*, 2nd edn. Wiley, New York, 1993.
15. Abramowitz, Milton and Stegun, Irene A., *Handbook of Mathematical Functions*. Dover Publications, New York, 1972.
16. Beck, James V. and Arnold, Kenneth J., *Parameter Estimation in Engineering and Science*. Wiley, New York, 1977.
17. Walter, E. and Pronzato, L., *Identification de Modèles Paramétriques à Partir de Données Expérimentales*. Masson, Paris, 1994.
18. Candy, James V., *Signal Processing: The Model-Based Approach*. McGraw-Hill, New York, 1986.

APPENDIX

A. *Exponential approximation of* $\theta_i^*(r, t)$

Consider a cylindrical sample of thickness L, radius R, thermal diffusivity α and thermal conductivity λ. Initially, the sample is at zero temperature and absorbs, at its front face, an azimuthal symmetric pulse with the energy distribution $Qf(r)$. It is further assumed that, for time $t > 0$, the sample dissipates heat at all boundary surfaces into the environment. The temperature rise at the rear face is given by the Green's function solution equation:

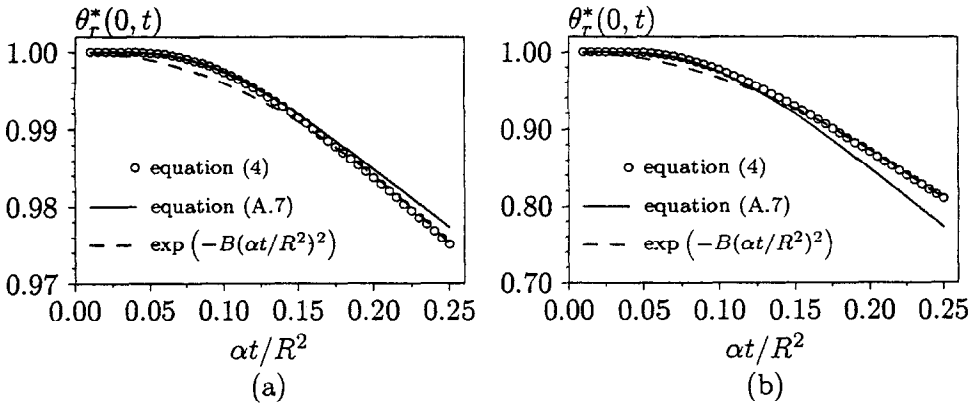

Fig. A1. Temperature at the center of the cylinder: (a) $Bi = 0.1$; (b) $Bi = 1$.

$$T(r,t) = \frac{\alpha}{\lambda}\int_{\tau=0}^{t}\int_{r'=0}^{R} G_{Z33}(e,t\,|\,0,\tau)G_{R03}(r,t\,|\,r',\tau) \times Qf(r')\delta(\tau)2\pi r'\,dr'\,d\tau \quad \text{(A1)}$$

where $G_{Z33}(\cdot)$ and $G_{R03}(\cdot)$ are the Green's function in the axial and radial coordinates [13, Appendix R and X]. Let θ^* be the dimensionless temperature defined as $\theta^* = \lambda LT/Q\alpha$. Equation (A1) becomes:

$$\theta(r,t) = LG_{Z33}(L,t\,|\,0,0) \times \underbrace{\int_{r'=0}^{R} G_{R03}(r,t\,|\,r',0)Qf(r')2\pi r'\,dr'}_{\theta_r^*} \quad \text{(A2)}$$

The component $LG_{Z33}(\cdot)$ has been already given for small times (equation (9)). The general solution for θ_r^* is given by equation (4).

It is obvious from equation (A2) that θ_r^* is equivalent to the dimensionless temperature of a solid cylinder initially at temperature $f(r)$ whose lateral boundary surface dissipates heat into a medium at zero temperature for time $t > 0$. The mathematical formulation of this problem can be written in the following differential form:

$$\begin{cases} \dfrac{\partial^2\theta_r^*}{\partial r^2} + \dfrac{1}{r}\dfrac{\partial\theta_r^*}{\partial r} = \dfrac{1}{\alpha}\dfrac{\partial\theta_r^*}{\partial t}: & t > 0, 0 \leqslant r < R \\ \dfrac{\partial\theta_r^*}{\partial r} + H\theta_r^* = 0: & t > 0, r = R, H = h/\lambda \\ \theta_r^* = f(r): & t = 0, 0 \leqslant r < R \end{cases} \quad \text{(A3)}$$

The Laplace transform of equation (A3) is given by:

$$\begin{cases} \dfrac{d^2\tilde{\theta}_r^*}{dr^2} + \dfrac{1}{r}\dfrac{d\tilde{\theta}_r^*}{dr} = \dfrac{1}{\alpha}[s\tilde{\theta}_r^* - f(r)] & 0 \leqslant r < R \\ \dfrac{d\tilde{\theta}_r^*}{dr} + H\tilde{\theta}_r^* = 0 & r = R \end{cases} \quad \text{(A4)}$$

where s is the Laplace transform variable.

In the special case of $f(r) = 1$, the solid cylinder is initially at uniform temperature, which also means that the pulse absorbed by the sample is uniformly distributed. The solution in the Laplace domain becomes:

$$\tilde{\theta}_r^*(r,s) = \frac{1}{s} - \frac{BiI_0(qr)}{s[BiI_0(qR) + qRI_1(qR)]} \quad \text{(A5)}$$

with $Bi = hR/\lambda$ (Biot number) and $q = \sqrt{s/\alpha}$. It is now of interest to find a solution at the center of the cylinder that converges rapidly for small times. This is obtained by setting $r = 0$ and performing the asymptotic expansion of equation (A5) for large values of q:

$$\tilde{\theta}_r^*(0,s) = \frac{1}{s} - \frac{Bi\sqrt{2\pi}\alpha^{1/4}}{\sqrt{R}}\left[\frac{\exp(-qR)}{s^{5/4}} + \cdots,\right]. \quad \text{(A6)}$$

The term by term inversion of equation (A6) gives the solution in the time domain:

$$\theta_r^*(0,t) = 1 + \frac{Bi\sqrt{2\pi}}{\Gamma\left(\frac{3}{4}\right)}\left[\frac{{}_1F_1\left(\frac{1}{4};\frac{3}{2};-\frac{R^2}{4\alpha t}\right)}{\left(\frac{\alpha t}{R^2}\right)^{1/4}} - \frac{\sqrt{\pi}L_{1/4}^{(-1/2)}\left(-\frac{R^2}{4\alpha t}\right)}{\left(\frac{\alpha t}{R^2}\right)^{-1/4}}\right] + \cdots, \quad \text{(A7)}$$

where ${}_1F_1(\cdot)$ is the hypergeometric Kummer confluent function [15, Chap. 13] and $L_{(\cdot)}^{(\cdot)}(\cdot)$ the generalized Laguerre polynomial [15, Chap. 22]. Replacing these functions with their asymptotic expansions for $t \to 0$, equation (A7) becomes a polynomial that is similar to the Taylor series expansion of an exponential function:

$$\theta_r^*(0,t) = 1 + \sum_{n=1}^{\infty} a_n\left(\frac{\alpha t}{R^2}\right)^n + \cdots,$$

$$\theta_r^*(0,t) = \exp(-B(\alpha t/R^2)^m) + \cdots. \quad \text{(A8)}$$

where B and m are unknown parameters.

The adequation of the function $\exp(-B(\alpha t/R^2)^2)$ as the radial component of the temperature at the center of the sample is shown in Fig. A1. Starting from equation (A8), we set $m = 2$ and identify the parameter B on the basis of true values obtained with equation (4). The errors arising from the exponential approximation are relatively low.

B. *Moment method adapted to* $R^* = 1$

The moment method is based on a relation between two temporal moments of the thermogram: m_0^* (order 0) and m_{-1}^* (order -1). The relation proposed by the authors is an approximation for different values of R^* and Bi [9]. Performing the same calculations for the special case $R^* = 1$, we obtain the following relation:

$$m_0^* = 0.08576 - 0.32852(0.54866 - m_{-1}^*) + 0.27923(0.54866 - m_{-1}^*)^2 \quad \text{(B1)}$$